DOUBLY STRATIFIED EFFECTS IN A FREE CONVECTIVE FLOW OVER A VERTICAL PLATE WITH HEAT AND MASS TRANSFER

by

Ganesan PERIYANAGOUNDER*, Suganthi Renugopal KANNIAPPAN, and Loganathan PARASURAMAN

Department of Mathematics, Anna University, Chennai, India

Original scientific paper
DOI: 10.2298/TSCI11006202P

An analysis is performed to study the effects of thermal and mass stratification in a transient free convective flow of a viscous, incompressible fluid past an isothermal vertical plate. The governing boundary layer equations are solved numerically using an implicit finite difference scheme of Crank-Nicolson type. The doubly stratified effects on the velocity, temperature, and concentration are shown graphically. It is observed that an increase in thermal stratification parameter decreases the velocity, temperature profiles and increases the concentration profiles. As well, increase in mass stratification parameter decreases the velocity, concentration profiles and increases the temperature profiles. Also, the influence of the thermal and mass stratification parameter on local as well as average skin-friction, the rate of heat and mass transfer are discussed and presented graphically. The results are compared with particular solutions available in the literature. The present results are found to be in good agreement with the existing particular solution of the problem.

Key words: *transient, isothermal, thermal stratification, mass stratification, buoyancy*

Introduction

Natural convective flow caused by combined buoyancy effects of thermal and mass diffusion has been analyzed by many authors. It has enormous applications in various industries and environments such as nuclear power plants, polymer production, chemical catalytic reactors, food processing and geophysical flows etc. The problem of transient free convective flow past a semi-infinite vertical isothermal plate was first studied by Siegel [1]. Later, Hellums and Churchill [2], and Callahan and Marner [3] examined the problem of free convective flow past a vertical plate using an explicit finite difference scheme. Gebhart and Pera [4] analyzed the nature of vertical natural convection flows resulting from the combined buoyancy effects of thermal and mass diffusion. Soundalgekar and Ganesan [5] investigated the problem of transient free convective flow over an isothermal vertical plate by employing an implicit finite difference scheme of Crank-Nicolson type. Later on, many authors widened the field by considering the in-

* Corresponding author; e-mail: ganesan@annauniv.edu

fluence of the other factors such as radiation, chemical reaction, MHD, *etc*. in a free convective flow. In a similar manner, Ogulu and Makinde [6] investigated analytically the thermal radiation effects on an unsteady, free convective flow past a vertical plate in the presence of magnetic field and constant heat flux. Shyam Sundar Tak *et al.* [7] and Makinde [8] analyzed the Soret and Dufour effects about a vertical surface embedded in a porous medium. Makinde and Olanrewaju [9] studied the unsteady mixed convection flow past a vertical porous flat plate moving through a binary mixture in the presence of radiative heat transfer and n^{th}-order Arrhenius type of irreversible chemical reaction with Dufour and Soret effects. Makinde [10] studied the problem of free convective flow over a semi-infinite moving vertical plate in the presence of internal heat generation and a convective surface boundary condition.

Similar to the above seen factors that influence the heat and mass transfer processes, the effect of stratification is also one of the important aspects that have to be taken into account in the study of heat and mass transfer. Stratification of fluids occurs mainly because of either temperature variations or concentration differences or due to presence of different fluids having different densities. The notion of stratification is important in lakes and ponds. It is vital to monitor the temperature stratification and concentration differences of hydrogen and oxygen in such environments as it directly affects the growth rate of all cultured species. To study the thermal stratification in water pools containing several systems, Satishkumar *et al.* [11] experimented with a single strip heater immersed in a tank containing stratified fluid. Also, the analysis of thermal stratification is important for solar engineers because higher energy efficiency can be achieved with a better stratification. It has been shown by scientists that thermal stratification in energy store may considerably increase system performance.

Due to the immense importance of stratification, authors have analyzed the influence of thermal stratification on the rate of heat and mass transfer. Chen and Eicchorn [12] explored the natural convective flow over a heated vertical surface in a thermal stratified medium by using local non-similarity technique. Later, Srinivasan and Angirasa [13] and Angirasa and Srinivasan [14], focused on the combined heat and mass transfer effects in a thermally stratified medium using an explicit finite difference method. Saha and Hossain [15] examined combined buoyancy effects due to thermal and mass diffusion in thermally stratified media. Geetha and Moorthy [16] studied the variable viscosity, chemical reaction and thermal stratification effects on mixed convection heat and mass transfer along a semi-infinite vertical plate.

Though, all of the above studies analyze the effects in a thermally stratified medium, a very few analysis have been done to study the influence of thermal and mass stratification on heat and mass transfer by natural convective flow. Barahim *et al.* [17] study shows that during the strongest period of stratification, the dissolved oxygen content was found to diminish significantly with the depth while iron and manganese were recorded at the highest concentration in a reservoir located in Malaysia. Rathish Kumar and Gupta [18] considered the problem of non-Darcian combined heat and mass transfer from a vertical wavy wall in a doubly stratified porous medium and solved numerically by local non-similarity technique. Hence, in certain cases, consideration of mass stratification could cause significant changes and it may not be negligible. This kind of model may be used in the analysis of electrolytic cell, nuclear waste management, cooling of electronic devices, cooling of extruded polymers after dyeing, *etc*. If the case of lead acid batteries is taken as an example, ambient temperature conditions can cause temperature stratification in it. Also, as a typical lead-acid battery contains a mixture with varying concentrations of water and acid, a slight difference in density between water and acid can occur and that might result in concentration stratification. As well, temperature stratification

within very large batteries could produce internal leakage or self-discharge. Concentration stratification for a longer period of time can result in the sediments being formed at the bottom of the plates, while the upper portions remaining in relatively good shape. This stratification would reduce battery life and its capacity.

The aim of the present work is to study the influence of thermal and mass stratification in a free convective flow past a semi-infinite vertical plate by employing an implicit finite difference scheme of Crank-Nicolson type. Stratification effects on velocity, temperature and concentration profiles are presented graphically. Also the effects of parameters on the rate of heat and mass transfer are discussed. The results are compared with the particular solutions obtained by Gebhart *et al.* [4] and Srinivasan *et al.* [13] using analytical method and explicit finite difference method respectively. They are found to be in good agreement.

Mathematical analysis

A 2-D transient, laminar free convective flow of a viscous incompressible stratified fluid past a semi-infinite isothermal vertical plate is considered. Initially, the fluid and the plate are assumed to be at the same temperature T_∞ and concentration C_∞. For time period $t' > 0$ the temperature of the plate raise to T_w, as well as concentration level near the plate raisis to C_w. In the ambient, the temperature and concentration increases linearly with height, where $T_{\infty,0}$ and $C_{\infty,0}$ being its values at $x = 0$, respectively. All the fluid physical properties are assumed to be constant except the body force terms. In the present analysis viscous dissipation, chemical reaction and Joule's heating effect are assumed to be negligible. The x-axis is taken along the plate in the vertically upward direction and the y-axis is taken normal to the plate as shown in fig. 1.

Under the above assumptions, the governing boundary layer equations for the flow with usual Boussinesq's approximation [19]:

$$\frac{\partial u}{\partial x} + \frac{\partial v}{\partial y} = 0 \tag{1}$$

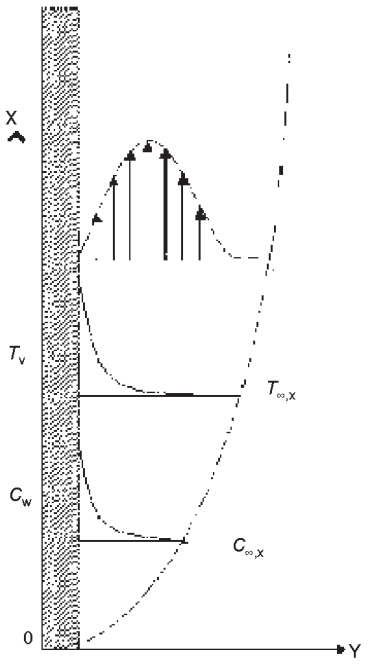

Figure 1. Schematic diagram

$$\frac{\partial u}{\partial t'} + u\frac{\partial u}{\partial x} + v\frac{\partial u}{\partial y} = \upsilon\frac{\partial^2 u}{\partial x^2} + g\beta(T' - T_{\infty,x}) + g\beta^*(C' - C_{\infty,x}) \tag{2}$$

$$\frac{\partial T'}{\partial t'} + u\frac{\partial T'}{\partial x} + v\frac{\partial T'}{\partial y} = \alpha\frac{\partial^2 T'}{\partial y^2} \tag{3}$$

$$\frac{\partial C'}{\partial t'} + u\frac{\partial C'}{\partial x} + v\frac{\partial C'}{\partial y} = D\frac{\partial^2 C'}{\partial y^2} \tag{4}$$

The initial and boundary conditions are:

$$\begin{aligned}
&t' \le 0, \quad u = 0, \quad v = 0, \quad T' = T_{\infty,\mathrm{x}}, \quad C' = C_{\infty,\mathrm{x}} \\
&t' > 0, \quad u = 0, \quad v = 0, \quad T' = T_{\mathrm{w}}, \quad C' = C_{\mathrm{w}} \quad \text{at} \quad y = 0 \\
&\qquad\quad u = 0, \quad v = 0, \quad T' = T_{\infty,0}, \quad C' = C_{\infty,0} \quad \text{at} \quad x = 0 \\
&\qquad\quad u \to 0, \qquad\quad T' = T_{\infty,\mathrm{x}}, \quad C' \to C_{\infty,\mathrm{x}} \quad \text{as} \quad y \to \infty
\end{aligned} \tag{5}$$

Introducing the non-dimensional quantities:

$$X = \frac{x}{L},\ Y = \frac{y}{L}\sqrt[4]{\mathrm{Gr}},\ U = \frac{uL}{\upsilon}\frac{1}{\sqrt{\mathrm{Gr}}},\ V = \frac{vL}{\upsilon}\frac{1}{\sqrt[4]{\mathrm{Gr}}},\ T = \frac{T' - T_{\infty,x}}{T_{\mathrm{w}} - T_{\infty,0}},\ C = \frac{C' - C_{\infty,x}}{C_{\mathrm{w}} - C_{\infty,0}}$$

$$t = \frac{t'\upsilon}{L^2}\sqrt{\mathrm{Gr}},\ \mathrm{Gr} = \frac{\mathrm{g}\beta L^3 (T_{\mathrm{w}} - T_{\infty,0})}{\upsilon^2},\ \mathrm{Gr} = \frac{\mathrm{g}\beta^* L^3 (C_{\mathrm{w}} - C_{\infty,0})}{\upsilon^2},\ N = \frac{T_{\mathrm{w}} - T_{\infty,0}}{C_{\mathrm{w}} - C_{\infty,0}}$$

$$S_{\mathrm{T}} = \frac{\dfrac{\mathrm{d}T_{\infty,x}}{\mathrm{d}X}}{T_{\mathrm{w}} - T_{\infty,0}},\ S_{\mathrm{M}} = \frac{\dfrac{\mathrm{d}C_{\infty,x}}{\mathrm{d}X}}{C_{\mathrm{w}} - C_{\infty,0}},\ \alpha = \frac{k}{\rho c_p},\ \mathrm{Sc} = \frac{\upsilon}{D},\ \mathrm{Pr} = \frac{\upsilon}{\alpha}$$

Equations (1), (2), (3), and (4) reduce to following non-dimensional form:

$$\frac{\partial U}{\partial X} + \frac{\partial V}{\partial Y} = 0 \tag{6}$$

$$\frac{\partial U}{\partial t} + U\frac{\partial V}{\partial X} + V\frac{\partial V}{\partial Y} = \frac{\partial^2 U}{\partial Y^2} + T + NC \tag{7}$$

$$\frac{\partial T}{\partial t} + U\frac{\partial T}{\partial X} + V\frac{\partial T}{\partial Y} = \frac{1}{\mathrm{Pr}}\frac{\partial^2 T}{\partial Y^2} - S_{\mathrm{T}}U \tag{8}$$

$$\frac{\partial C}{\partial t} + U\frac{\partial C}{\partial X} + V\frac{\partial C}{\partial Y} = \frac{1}{\mathrm{Sc}}\frac{\partial^2 C}{\partial Y^2} - S_{\mathrm{M}}U \tag{9}$$

The boundary condition for temperature and concentration along the wall in non-dimensional form are obtained as:

$$T = 1 - \frac{T_{\infty,x} - T_{\infty,0}}{T_w - T_{\infty,0}}$$

as $T_{\infty,\mathrm{x}}$, and $C_{\infty,\mathrm{x}}$ are linear functions of x,

$$T = 1 - \frac{1}{T_{\mathrm{w}} - T_{\infty,0}}\frac{\mathrm{d}T_{\infty,x}}{\mathrm{d}X}X = 1 - S_{\mathrm{T}}X$$

where $S_{\mathrm{T}} = (\mathrm{d}T_{\infty,\mathrm{x}}/\mathrm{d}X)/(T_{\mathrm{w}} - T_{\infty,0})$ is the thermal stratification parameter.

Similarly,

$$C = 1 - \frac{1}{C_{\mathrm{w}} - C_{\infty,0}}\frac{\mathrm{d}C_{\infty,x}}{\mathrm{d}X}X = 1 - S_{\mathrm{M}}X$$

where $\mathrm{S_M} = (\mathrm{d}C_{\infty,\mathrm{x}}/\mathrm{d}X)/(C_{\mathrm{w}} - C_{\infty,0})$ is the mass stratification parameter.

For linear stratification, T_{S} and M_{S} are constants and for other variations it can be represented as a function of x.

Thus, the boundary conditions (5) reduces as:

$$t \le 0, \quad U = 0, \quad V = 0, \quad T = 0, \quad C = 0$$

$$\begin{aligned} t>0,\ & U=0, \quad V=0, \quad T=1-S_T X, \quad C=1-S_M X \quad \text{at} \quad Y=0 \\ & U=0, \quad V=0, \quad T=0, \qquad\ C=0 \qquad\ \text{at} \quad X=0 \\ & U\to 0, \qquad\ T\to 0, \qquad\ C\to 0 \qquad\ \text{as} \quad Y\to\infty \end{aligned} \tag{10}$$

The local as well as average values of skin friction, Nusselt number, and Sherwood number in dimensionless form are as follows.

The shear stress at the plate is defined as:

$$\tau_x = \mu \left.\frac{\partial u}{\partial y}\right|_{y=0} \tag{11}$$

Introducing the non-dimensional quantities in eq. (11), the non-dimensional form of local skin friction is obtained as:

$$\tau_X = \sqrt[4]{\mathrm{Gr}^3} \left.\frac{\partial U}{\partial Y}\right|_{Y=0} \tag{12}$$

The average skin friction is given by:

$$\overline{\tau}_X = \sqrt[4]{\mathrm{Gr}^3} \int_0^1 \left.\frac{\partial U}{\partial Y}\right|_{Y=0} \mathrm{d}X \tag{13}$$

The Nusselt number is defined by:

$$\mathrm{Nu}_x = \frac{-x \left.\dfrac{\partial T'}{\partial y}\right|_{y=0}}{T_\mathrm{w} - T_{\infty,0}} \tag{14}$$

Using the non-dimensional quantities in eq. (14), the non-dimensional form of local Nusselt number is obtained as:

$$\mathrm{Nu}_X = -\sqrt[4]{\mathrm{Gr}} \frac{X \left.\dfrac{\partial T}{\partial Y}\right|_{Y=0}}{1-S_\mathrm{T} X} \tag{15}$$

The average Nusselt number is given by:

$$\overline{\mathrm{Nu}}_X = -\sqrt[4]{\mathrm{Gr}} \int_0^1 \frac{\left.\dfrac{\partial T}{\partial Y}\right|_{Y=0}}{1-S_\mathrm{T} X} \mathrm{d}X \tag{16}$$

The Sherwood number is defined by:

$$\mathrm{Sh}_x = \frac{-x \left.\dfrac{\partial C'}{\partial y}\right|_{y=0}}{C_\mathrm{w} - C_{\infty,\mathrm{x}}} \tag{17}$$

Using the non-dimensional quantities in eq. (17), the non-dimensional form of local Sherwood number is obtained as:

$$\overline{\mathrm{Sh}}_X = -\sqrt[4]{\mathrm{Gr}} \int_0^1 \frac{\left.\dfrac{\partial C}{\partial Y}\right|_{Y=0}}{1-S_\mathrm{M} X} \tag{18}$$

The average Sherwood number is given by:

$$\overline{\mathrm{Sh}}_X = -\sqrt[4]{\mathrm{Gr}} \int_0^1 \frac{\left.\dfrac{\partial T}{\partial Y}\right|_{Y=0}}{1 - S_M X} \mathrm{d}X \tag{19}$$

The derivatives involved in eqs. (12), (13), (15), (16), (18), and (19) are evaluated by using a five-point approximation formula and the integrals are evaluated by Newton-Cotes closed integration formula.

Numerical procedure

The 2-D, non-linear, coupled partial differential eqs. (6)-(9) under the initial and boundary conditions (10) are solved using implicit finite difference scheme of Crank-Nicolson type which converges faster and also unconditionally stable.

The region of integration is considered as a rectangle with sides $X\max = 1$ and $Y\max = 14$, where $Y\max$ corresponds to $Y = \infty$. The max Y was chosen as 14 after some preliminary investigations so that the last two of the boundary conditions of (10) are satisfied. Here, the subscript i assigns the grid point along X-direction, j along Y-direction, and k along t direction. The mesh sizes are taken as $\Delta X = 0.05$, $\Delta Y = 0.25$ with time step $\Delta t = 0.01$. The equations at every internal nodal point for a particular i-level constitute a tridiagonal system. This system is solved by applying Thomas algorithm as described in Carnahan *et al*. [20]. Thus the values of C, T, U, and V are known at all nodal points in the rectangular region at $(k + 1)^{\text{th}}$ time level by repeating the procedure for various i-levels. Computations are carried out for all the time levels until the steady-state is reached. The steady-state solution is assumed to have been reached, when the absolute difference between the values of U, as well as temperature T, and concentration C at two consecutive time steps are less than 10^{-5} at all grid points.

The scheme is proved to be unconditionally stable using Von-Neumann technique, as shown by Soundalgekar and Ganesan [5]. The local truncation error is $o(\Delta t^2 + \Delta X + \Delta Y^2)$ and it tends to zero as Δt, ΔX, and ΔY tend to zero. Hence the scheme is compatible. Stability and compatibility ensures the convergence of the scheme.

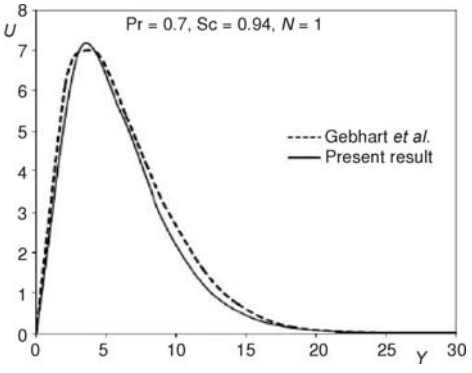

Figure 2. Comparison of velocity profiles

Results and discussion

In order to get a clear insight of the physical problem, numerical results are displayed with the help of graphical illustrations. The velocity, temperature and concentration of the fluid are shown graphically to observe the influence of parameters.

To check the accuracy of the result, the present solution is compared with the available particular solution in the literature. Figure 2 shows the comparison of velocity profiles for Pr = 0.7, Sc = 0.94, and $N = 1.0$ in the absence of thermal and mass stratification with particular solutions of Gebhart and Pera [4] whilst fig. 3 compares the temperature and concentration profiles for Pr = 0.7, Sc = 0.94, and $N = 1.0$ in the absence of mass stratification with the available particular solutions of Srinivasan and Angirasa [13]. From figs. 2 and 3, it is observed that the present results are in good agreement with the existing solution.

The effects of the thermal stratification level and mass stratification level have been analyzed on the double diffusive natural convection process for a range of thermal stratification and mass stratification, $0 \le S_T \le 1$and $0 \le S_M \le 1$, respectively. As at the lower end of the vertical wall ($X = 0$), due to the boundary condition $T = 1 - S_T X$, wall temperature is always 1, irrespective of the stratification parameter S_T. $S_T = 1$ shows that corresponding to the considered wall length $X(0 < X < 1)$, there is variation in the temperature from $T = 1$ at the lower end ($X = 0$) to $T = 0$ at the upper end ($X = 1$) of the vertical surface. It is observed that for $S_T = 1$ the temperature in the ambient equals the surface temperature at $X = 1$ and for a value of $S_T > 1$, a portion at the top of the surface will have a temperature less than the ambient. For the investigation, the Prandtl number was taken to be Pr = 0.73 which corresponds to air; the values of Schmidt number (Sc) were chosen to be Sc = 0.2 and 0.6 representing diffusing chemical species of most common interest in air like H_2, H_2O, respectively. The velocity, temperature and concentration profiles are analysed at the leading edge of the plate $X = 1$.

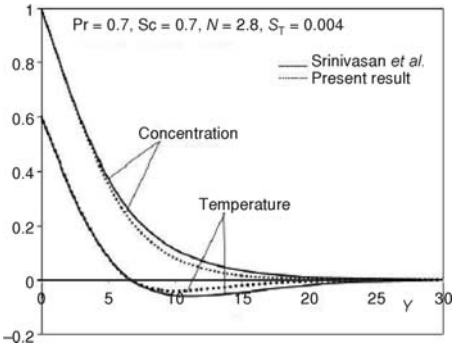

Figure 3. Comparison of temperature and concentration profiles

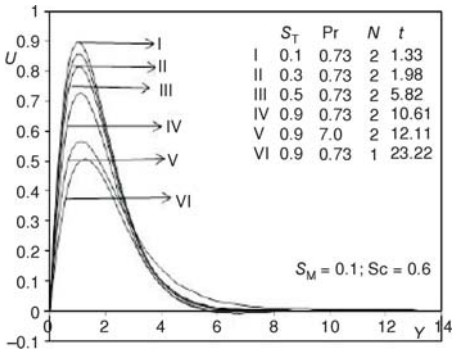

Figure 4. Velocity profiles for different S_T, Pr, and N

It is examined from fig. 4 and fig. 5 that an increase in thermal stratification parameter S_T, decreases the velocity and temperature profiles. Increase in thermal stratification parameter reduces the temperature difference between the ambient and the surface. This factor causes a decrease in the buoyancy force which decelerates the velocity of the flow. The deceleration in the velocity in turn reduces the temperature profiles. Also, from fig. 6, it is noted that an increase in S_T, increases the concentration. This is because thermal strat-

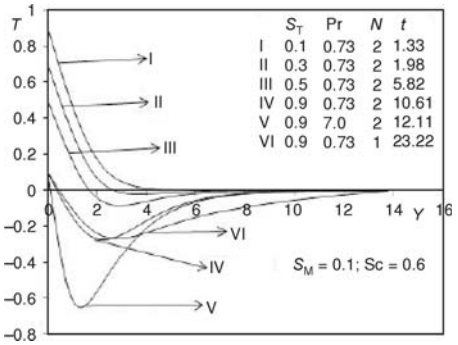

Figure 5. Temperature profiles for different S_T, Pr, and N

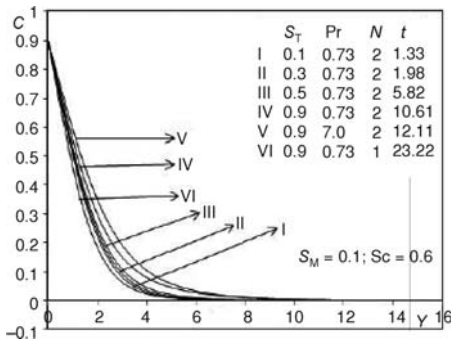

Figure 6. Concentration profiles for different S_T, Pr, and N

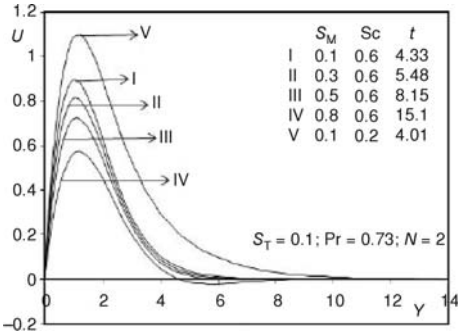

Figure 7. Velocity profiles for different S_M and Sc

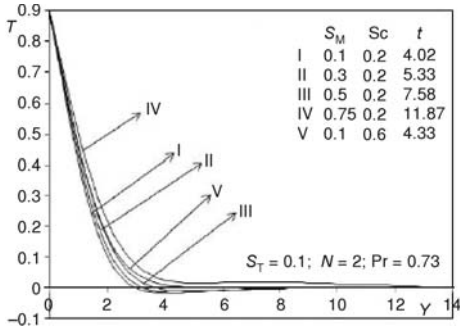

Figure 8. Temperature profiles for different S_M and Sc

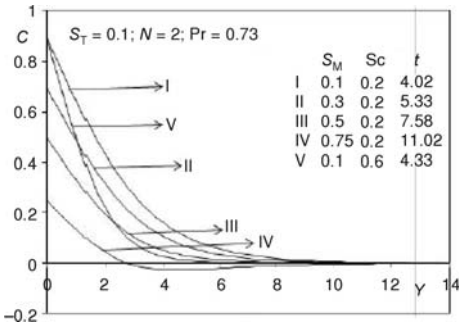

Figure 9. Concentration profiles for different S_M and Sc

ification suppresses the thermal buoyancy with the resultant decrease in velocity and temperature, consequently the concentration level increases.

Figures 7 and 9 describe that an increase in mass stratification parameter decreases the velocity and concentration profiles. Increase in mass stratification parameter decreases the concentration gradient between the ambient and the surface. As an aiding buoyancy flow been considered, reduction in the concentration gradient reduces the buoyancy force which decelerates the velocity of the flow. From fig. 8, it is observed that an increase in S_M, increases the temperature profiles.

Figure 7 depicts that an increase in Schmidt number decreases the velocity. This is due to the fact that a larger Sc corresponds to a concentration boundary layer relative to the momentum boundary layer and hence, for a fixed Prandtl number, an increase in Sc leads to a fall in velocity. Since the velocity drops considerably with increasing Schmidt number, there is a smaller quantity of cold fluid coming up from below to a warmer ambient. Hence the fluid in the boundary layer is warmer with a higher Schmidt number as seen from fig. 8. As well, fig. 9 represents that a fluid with higher Schmidt number has a smaller value of the species diffusion coefficient; consequently, its concentration level decreases as seen from eq. (9).

As Prandtl number is characteristic of the relationship between the momentum boundary layer thicknesses to thermal boundary layer thickness, the thermal boundary layer becomes thin by increasing the Pr as seen by fig. 5. The heat diffusion becomes slow due to an increase in Prandtl number which in turn reduces the velocity of the flow as noted in fig. 4. Figure 6 show that an increase in Pr increases the concentration. As high Prandtl fluid has low velocity, which in turn also implies that at lower fluid velocity the species diffusion is comparatively lower and hence higher species concentration is observed at high Prandtl number.

Figure 5 shows that by increasing the buoyancy ratio parameter N, the temperature initially drops and then rises. It is also observed from fig. 4 that the velocity increases with an increase in N. Buoyancy ratio parameter is defined as the ratio of mass diffusion force to thermal diffusion force. As a positive buoyancy ratio parameter is be-

ing considered here, the mass diffusion force aids the thermal diffusion force and hence an increase in the velocity of the flow.

Figures 10, 11, and 12 depict the velocity, temperature and concentration profiles at different time in the presence of doubly stratified effects. From the figures, it is observed that the velocity, temperature and concentration profile increases with the time t and after certain time step the profiles decreases gradually to attain the steady-state. Thus, during the transient flow development the boundary layer thickness for a time exceeds the steady-state value.

From figs. 13 and 16, it is noted that an increase in S_T, decreases the local and average skin friction. This is because, the velocity of the fluid decreases by increasing the stratification parameter as depicted in fig. 4. Therefore, there is a reduction in the shear stress along the wall and hence a decrease in the skin friction. Figures 14 and 15 depict that an increase in thermal stratification decreases the local Nusselt number and local Sherwood number. Figure 6 depicts that for a fixed S_M, an increase in thermal stratification parameter increases the concentration level in the fluid. This leads to a decrease in the concentration gradient and hence a subsequent decrease in the local Sherwood number. Similarly, from fig. 5, it is clear that the temperature decreases with an increasing stratification parameter. Thus, the temperature gradient along the wall increases and hence there is an increase in the average Nusselt number as seen from fig. 17. Also, it is noted that the influence of the mass stratification parameter on average Nusselt number is less significant.

Figures 13 and 16 represent that an increase in S_M, decreases the local and average skin friction. This is because, the velocity of the fluid decreases by increasing the mass stratification parameter as shown from fig. 7. The deceleration in the velocity reduces the wall friction and hence a decrease in the local and average skin friction. From figs. 15 and 18, it is observed that an increase in mass stratification increases the local and average Sherwood number. An increase in mass stratification parameter decreases the concentration as seen from fig. 9 which in turn increases the concentration gradient and results in an increase in the local as well the average Sherwood number.

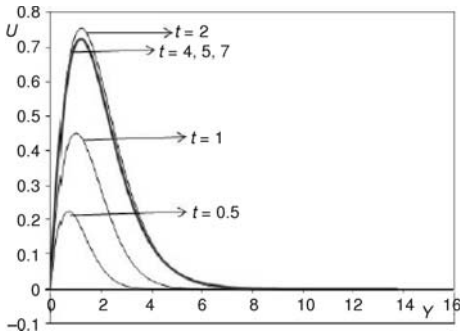

Figure 10. Velocity profiles for various time

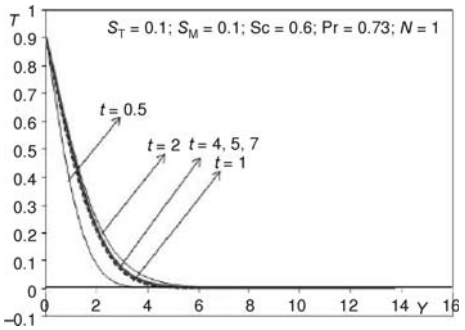

Figure 11. Concentration profiles for various time

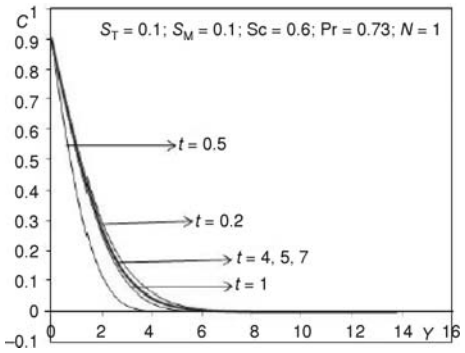

Figure 12. Concentration profiles for various time

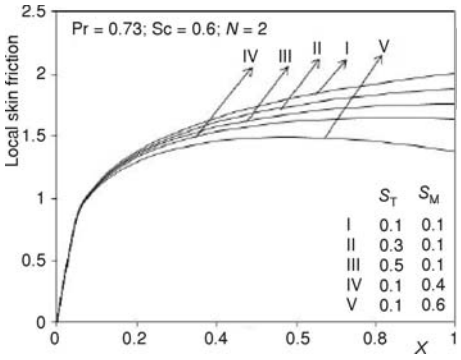

Figure 13. Local skin friction for different S_T and S_M

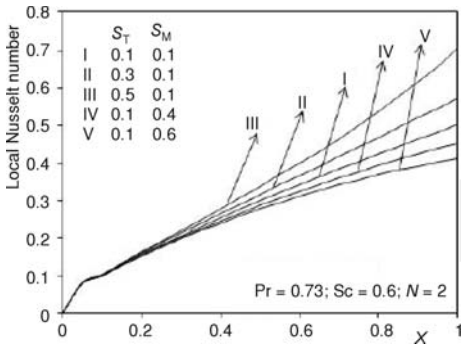

Figure 14. Local Nusselt number for different S_T and S_M

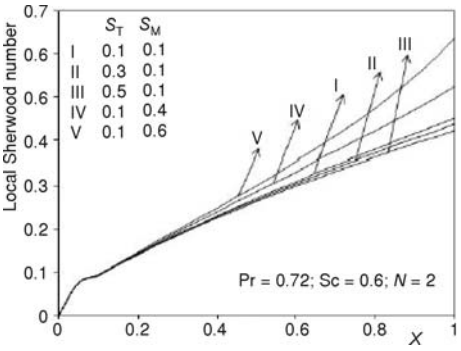

Figure 15. Local Sherwood number for different S_T and S_M

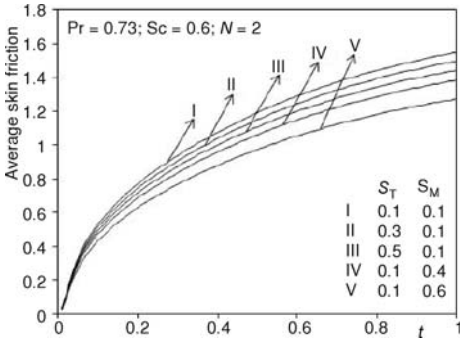

Figure 16. Average skin friction for different S_T and S_M

Figures 14 and 17 illustrate that an increase in mass stratification parameter decreases the local and average Nusselt number. Moreover, it is observed that the effect of thermal stratification parameter on average Sherwood number is not of much significance.

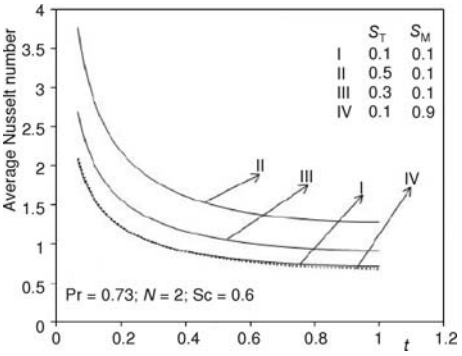

Figure 17. Average Nusselt number for different S_T and S_M

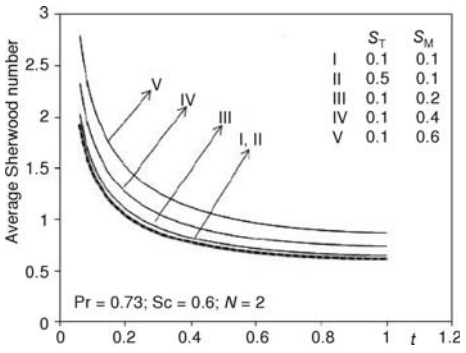

Figure 18. Average Sherwood number for different S_T and S_M

Conclusions

In the present work, a numerical study of free convective flow past a vertical plate in a doubly stratified medium has been analyzed. The dimensionless governing equations are solved by an implicit finite difference scheme of Crank-Nicolson type. The results reported in this paper were validated by comparing them with the particular solutions existing in the previously published paper. Our results show an excellent agreement with the existing work in the literature. The results are summarized as follows.

- Increase in thermal stratification parameter decreases the velocity and temperature profiles while it increases the concentration profiles.
- Increase in mass stratification parameter decreases the velocity and concentration profiles and increases the temperature profiles.
- An increase in buoyancy ratio parameter increases the velocity and decreases the temperature profiles.
- An increase in Schmidt number increases the temperature and decreases the velocity and concentration level.
- During the transient flow development, the momentum, thermal and concentration boundary layer thickness for a certain time exceeds the steady-state.
- Local and average values of skin friction and Sherwood number decrease by increasing the thermal stratification parameter. However, an opposite effect is observed for average Nusselt number.
- Local and average values of skin friction and Nusselt number decrease by increasing the mass stratification parameter. However, an opposite effect is observed for local and average Sherwood number.
- At an initial stage, only heat conduction (or) mass diffusion occurs.

Nomenclature

C – dimensionless concentration
C' – concentration in the fluid, [kgm^{-3}]
D – mass diffusion coefficient, [m^{2}s^{-1}]
Gr – thermal Grashof number
k – thermal conductivity, [Wm^{-1}K^{-1}]
N – buoyancy ratio parameter
$\underline{\mathrm{Nu}}$ – local Nusselt number
$\overline{\mathrm{Nu}}_X$ – average Nusselt number
Pr – Prandtl number
$\underline{\mathrm{Sc}}$ – Schmidt number
$\overline{\mathrm{Sh}}_X$ – average Sherwood number
Sh_x – local Sherwood number
S_M – mass stratification parameter
S_T – thermal stratification parameter
T – dimensionless temperature
T' – temperature of the fluid, [K]
t – dimensionless time
t' – time, [s]
U – dimensionless velocity component along the X-direction
u – velocity component along the plate, [ms^{-1}]
V – dimensionless velocity component along Y-direction
v – velocity component normal to the plate, [ms^{-1}]
X – dimensionless spatial co-ordinate along the plate
x – spatial co-ordinate along the plate, [m]
Y – dimensionless spatial co-ordinate normal to the plate
y – spatial co-ordinate normal to the plate, [m]

Greek symbols

α – thermal diffusivity, [m^{-2}s^{-1}]
β – volumetric thermal expansion coefficient, [K^{-1}]
β^* – volumetric coefficient of expansion with concentration, [K^{-1}]
υ – kinematic viscosity, [m^{2}s^{-1}]
τ_X – local skin friction
$\overline{\tau}_X$ – average skin friction

Subscripts

w – conditions on the wall
∞ – free stream conditions

Reference

[1] Siegel, R., Transient Free Convection from a Vertical Flat Plate, *Trans. ASME, 80* (1958), pp. 347-359
[2] Hellums, J. D., Churchill, S. W., Transient and Steady State, Free and Natural Convection, Numerical Solutions, Part I, The Isothermal Vertical Plate, *A.I.CH.E. Jl., 8* (1962), 5, pp. 690-692
[3] Callahan, G. D., Marner, W. J., Transient Free Convection with Mass Transfer on an Isothermal Vertical Flat Plate, *Int. J. Heat Mass Transfer, 19* (1976), 2, pp. 165-174
[4] Gebhart, B., Pera, L., The Nature of Vertical Natural Convection Flows Resulting from the Combined Buoyancy Effects of Thermal and Mass Diffusion, *Int. J. Heat Mass Transfer, 14* (1971), 12, pp. 2025-2050
[5] Soundalgekar, V. M., Ganesan, P., Finite-Difference Analysis of Transient Free Convection with Mass Transfer on an Isothermal Vertical Flat Plate, *International Journal of Engineering Science, 19* (1981), 6, pp. 757-770
[6] Ogulu, A., Makinde, O. D., Unsteady Hydromagnetic Free Convection Flow of a Dissipative and Radiating Fluid Past a Vertical Plate with Constant Heat Flux, *Chemical Engineering Communications, 196* (2009), 4, pp. 454-462
[7] Tak, S. S., *et al*., MHD Free Convection-Radiation Interaction along a Vertical Surface Embedded in Darcian Porous Medium in Presence of Soret and Dufour's Effects, *Thermal Science, 14* (2010), 1, pp. 137-145
[8] Makinde, O. D., On MHD Mixed Convection with Soret and Dufour Effects Past a Vertical Plate Embedded in a Porous Medium, *Latin American Applied Research, 41* (2011), 1, pp. 63-68
[9] Makinde, O. D., Olanrewaju, P. O., Unsteady Mixed Convection with Soret and Dufour Effects Past a Porous Plate Moving through a Binary Mixture of Chemically Reacting Fluid, *Chemical Engineering Communications, 198* (2011), 7, pp. 920-938
[10] Makinde, O. D., Similarity Solution for Natural Convection from a Moving Vertical Plate with Internal Heat Generation and a Convective Boundary Condition, *Thermal Science, 15* (2011), Suppl. 1, pp. S137-S143
[11] Satishkumar, N. V., *et al.*, Thermal Stratification Studies Related to the Passive Decay Heat Removal System of Advanced Heavy Water Reactor, Bhabha Atomic Research Centre, Mumbai, India, 2005 http://www.iaea.org/OurWork/ST/NE/NENP/NPTDS/Downloads/SRCM_NCP_2005_AUG /sess3_phen1_vijayan.pdf
[12] Chen, C. C., Eichhorn, R., Natural Convection from a Vertical Surface to a Thermally Stratified Fluid, *ASME Journal of Heat Transfer, 98* (1976), 3, pp. 446-451
[13] Srinivasan, J., Angirasa, D., Numerical Study of Double-Diffusive Free Convection from a Vertical Surface, *Int. J. Heat Mass Transfer, 31* (1988), 10, pp. 2033-2038
[14] Angirasa, D., Srinivasan, J., Natural Convection Flows Due to the Combined Buoyancy of Heat and Mass Diffusion in a Thermally Stratified Medium, *ASME Journal of Heat Transfer, 111* (1989),3, pp. 657-663
[15] Saha, S. C., Hossain, M. A., Natural Convection Flow with Combined Buoyancy Effects Due to Thermal and Mass Diffusion in Thermally Stratified Media, *Non-Linear Analysis: Modelling and Control, 9* (2004), 1, pp. 89-102
[16] Geetha, P., Moorthy, M. B. K., Variable Viscosity, Chemical Reaction and Thermal Stratification Effects on Mixed Convection Heat and Mass Transfer along a Semi-Infinite Vertical Plate, *American Journal of Applied Sciences, 8* (2011), 6, pp. 628-634
[17] Baharim, N. H., *et al*., Effects of Thermal Stratification on the Concentration of Iron and Manganese in a Tropical Water Supply Reservoir, *Sains Malaysiana, 40* (2011), 8, pp. 821-825
[18] Rathish Kumar, B. V., Gupta, S., Combined Influence of Mass and Thermal Stratification on Double-Diffusion Non-Darcian Natural Convection from a Wavy Vertical Wall to Porous Media, *Journal of Heat Transfer, 127* (2005), 6, pp. 637-647
[19] Schlichting, H., *Boundary Layer Theory*, John Wiley and Sons, New York, USA, 1969
[20] Carnahan, B., *et al*., *Applied Numerical Methods*, John Wiley and Sons, New York, USA, 1969

Paper submitted: October 6, 2011
Paper revised: August 15, 2012
Paper accepted: October 26, 2012